Observational Study

Medicine®

OPEN

A novel immunogenomic prognostic signature in lung squamous carcinoma

Jili Hou, MD[a,*], Qiuying Zhong, MD[b]

Abstract

Lung squamous carcinoma (LUSC) is a common subtype of lung cancer with limited available therapy and is thus associated with poor survival. Immune infiltrating cells and immune-related genes (IRGs) play a key role in the clinical outcomes of LUSC. In the present study, we aimed to develop a potential immunogenomic prognostic signature for patients with LUSC. The transcriptional profiles of 501 LUSC samples from The Cancer Genome Atlas (TCGA) and 2498 IRGs from the ImmPort database were used to develop the signature by Cox regression analysis. Ten differentially expressed and survival-associated IRGs were used to develop the risk signature, which could serve as an independent prognostic and predictive factor for patients with LUSC. Furthermore, this risk signature correlated with overall survival and clinical features, including age, in patients with LUSC. In addition, we identified 25 transcription factors that may regulate 15 survival-associated IRGs, using a regulatory network. Collectively, this immunogenomic signature could be a robust prognostic tool for patients with LUSC and holds great promise as individualized immunotherapy for LUSC.

Abbreviations: APLN = apelin, CTLA-4 = cytotoxic T lymphocyte-associated antigen-4, DEGs = differentially expressed genes, FDR = false discovery rate, FGFR4 = fibroblast growth factor receptor 4, IRGs = immune-related genes, KEGG = Kyoto Encyclopedia of Genes and Genomes, LUSC = lung squamous carcinoma, NSCLC = non-small cell lung cancer, OS = overall survival, PD-1 = programmed death 1, SEMA4C = semaphorin 4C, TCGA = The Cancer Genome Atlas, TF = transcription factors, TIME = tumor immune microenvironment.

Keywords: immune gene, immune system gene, lung squamous carcinoma, prognostic signature, risk score

1. Introduction

Lung cancer is the most commonly diagnosed cancer and the leading cause of cancer-related mortality worldwide.[1] Nonsmall cell lung cancer (NSCLC) accounts for approximately 85% of lung cancer cases, of which lung squamous carcinoma (LUSC) is a common type.[2] Although recommended first-line therapy for LUSC involves combination chemotherapy, the survival benefit from specific chemotherapy remains unclear.[3] In addition, the advantages of targeted therapies against adenocarcinomas are limited in the treatment of LUSC. Thus, shifting concepts and innovative approaches are needed to detect, manage, and monitor this disease.

Recently, next-generation sequencing technology has uncovered genomic profiles of lung cancers, including LUSC. Patients with LUSC and known smoking habits show a high rate of genetic alteration,[4] and thus, are potentially immunogenic and show promise for treatment with novel immunotherapeutic agents. For example, immune checkpoint inhibitors such as programmed death 1 (PD-1) and cytotoxic T lymphocyte-associated antigen-4 (CTLA-4) have demonstrated safety and efficacy in the treatment of LUSC.[5,6] These findings highlight the potential of the tumor immune microenvironment (TIME) in establishing clinical biomarkers and developing individualized medicine. Numerous studies have underpinned the importance of immune infiltrating cells with regard to survival outcomes in patients with LUSC.[7–9] However, there is a lack of prognostic signatures in LUSC based on the immunogenomic landscape.

In this study, we employed transcriptome data from The Cancer Genome Atlas (TCGA) to construct an immunogenomic prognostic signature for LUSC. Furthermore, we explored the regulatory mechanisms of key immune-related genes (IRGs). Finally, we analyzed the correlation between the risk index and clinical features to evaluate the clinical significance of this signature.

Editor: Wenwen Zhang.

The transcriptomic and clinical data were downloaded from TCGA (https://portal.gdc.cancer.gov/).

All the data of this paper was obtained from the open-access online database, we did not get these data from patients directly, nor intervene these patients. So, the ethical approval was not necessary.

This article does not contain any studies with human or animal subjects.

There are no human subjects in this article and informed consent is not applicable.

The authors declare that they have no conflicts of interest.

The datasets generated during and/or analyzed during the current study are publicly available.

[a] *Department of Oncology, Zhuji People's Hospital of Zhejiang Province, The Zhuji Affiliated Hospital of Shaoxing University, Zhuji 311800,* [b] *Department of Geriatrics, The Sixth Hospital of Wuhan, Affiliated Hospital of Jianghan University, Wuhan 430000, P.R.China.*

[*] *Correspondence: Jili Hou, Department of Oncology, Zhuji People's Hospital of Zhejiang Province, The Zhuji affiliated Hospital of Shaoxing University, No.9 Jianmin Road, Zhuji 311800, P.R. China (e-mail: houjili@outlook.com).*

How to cite this article: Hou J, Zhong Q. A novel immunogenomic prognostic signature in lung squamous carcinoma. Medicine 2021;100:2(e24073).

Received: 26 July 2020 / Received in final form: 31 October 2020 / Accepted: 3 December 2020

http://dx.doi.org/10.1097/MD.0000000000024073

2. Materials and methods

2.1. Sample data

The transcriptomic and clinical data were downloaded from TCGA (https://portal.gdc.cancer.gov/). RNA-seq data, including 501 LUSC and 49 control samples, were obtained from TCGA to construct an immunogenomic prognostic signature. All the data of this paper were obtained from the open-access online database, and we did not get these data from patients directly, nor intervene these patients. So, the ethical approval was not necessary.

2.2. Differentially expressed IRGs

IRGs were downloaded from the ImmPort database (https://immport.niaid.nih.gov).[10] Differentially expressed genes (DEGs) from the datasets were analyzed using the edgeR

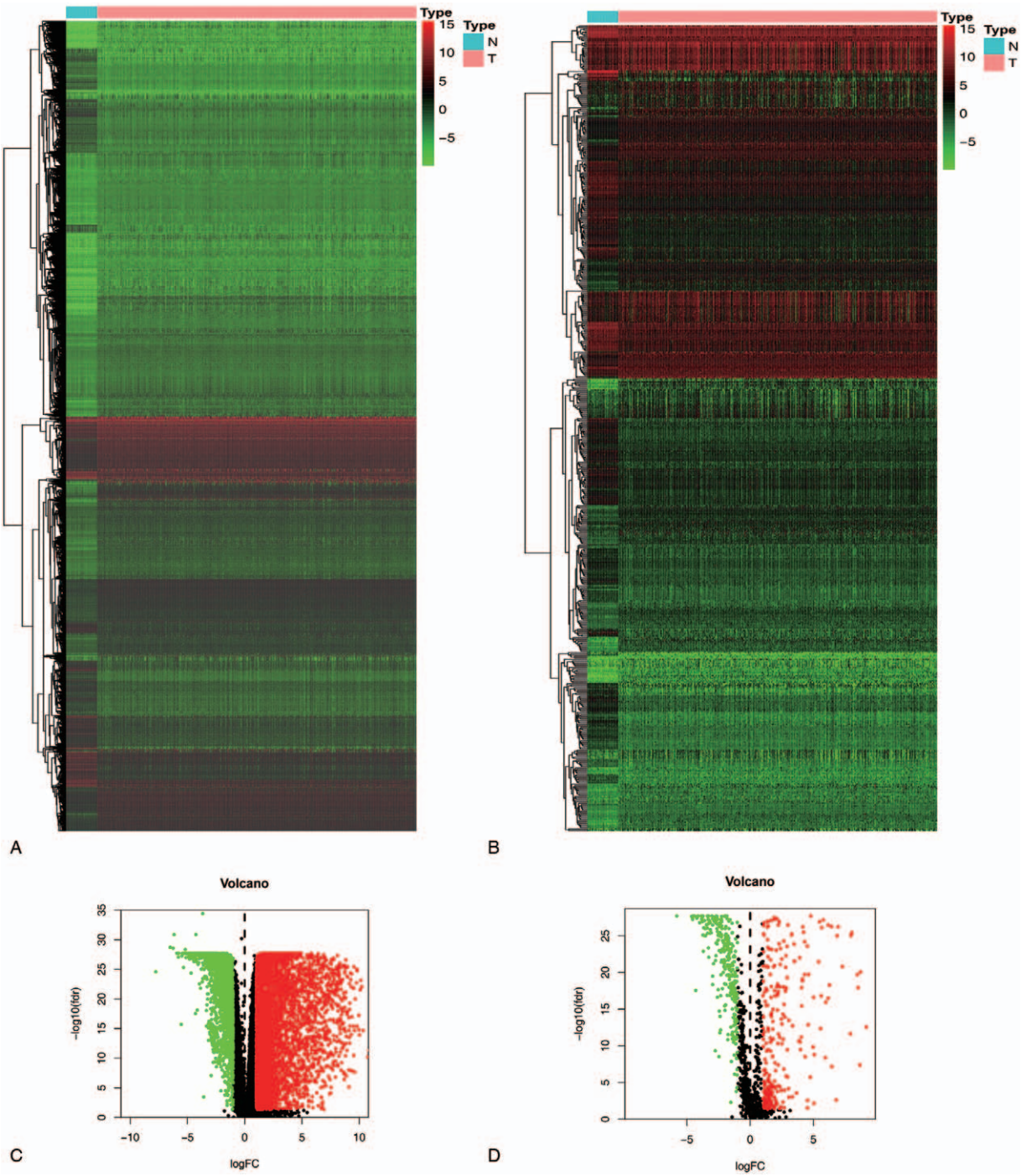

Figure 1. The differentially expressed genes. (A) Heatmap of differentially expressed genes in lung squamous carcinoma. (B) Heatmap of differentially expressed IRGs in lung squamous carcinoma. (C) Volcano plot of differentially expressed genes between lung squamous carcinoma and non-tumor tissues. (D) Volcano plot of differentially expressed IRGs between lung squamous carcinoma and non-tumor tissues. IRGs = immune-related genes.

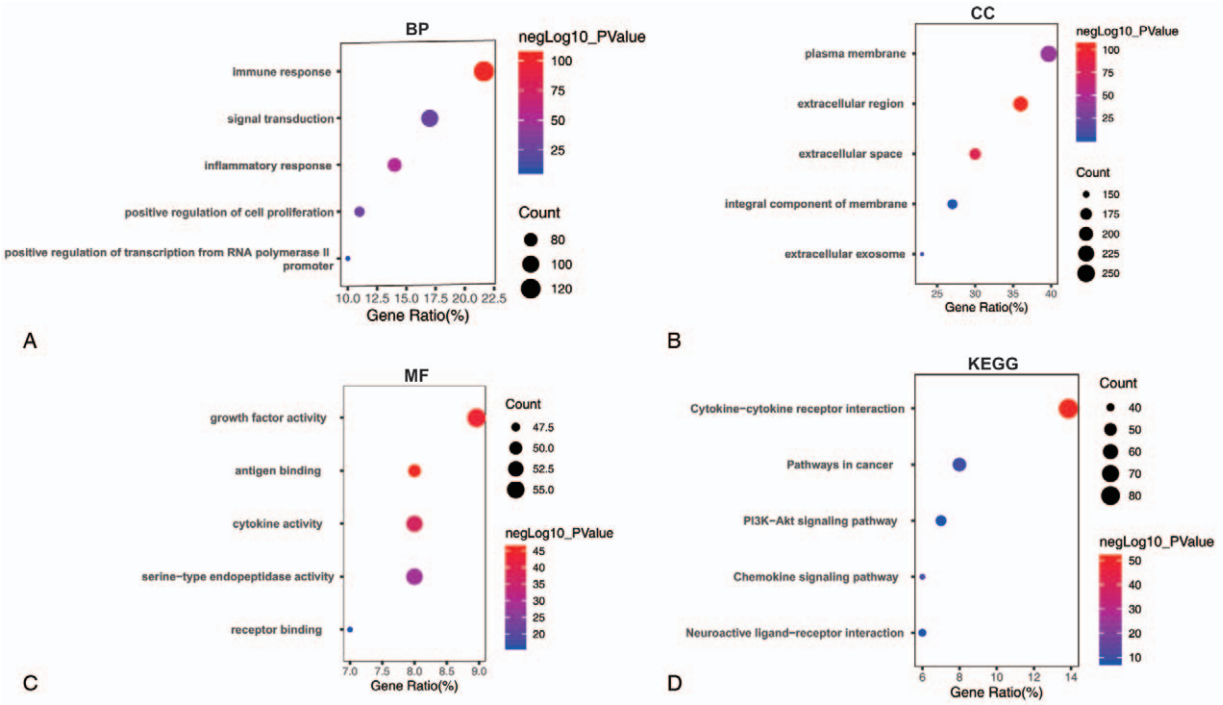

Figure 2. Functional enrichment analysis of differentially expressed IRGs. (A) Significantly enriched GO terms based on the biological process. (B) Significantly enriched GO terms based on the cellular component. (C) Significantly enriched GO terms based on molecular function. (D) Significantly enriched KEGG pathway. GO = gene ontology, IRGs = immune-related genes, KEGG = Kyoto Encyclopedia of Genes and Genomes.

package (http://bioconductor.org/packages/edgeR/). Differentially expressed IRGs were intersected with IRGs and DEGs. The absolute value of log fold change greater than 1 and a false discovery rate (FDR) value less than 0.05 were considered differentially expressed IRGs. Functional enrichment analysis was performed using the DAVID database to explore the molecular mechanisms of the identified genes.

2.3. Survival-associated IRGs

Differentially expressed IRGs with an FDR value of less than 0.01 were screened for the next analysis. Univariate Cox analysis was used to assess the relationship between identified IRGs and overall survival (OS) using the R survival package and visualized as a forest plot. In addition, genetic alteration of survival-associated IRGs was performed using cBioPortal for Cancer Genomics (http://www.cbioportal.org) database.[11]

2.4. Regulatory network of survival-associated IRGs

Transcription factors (TFs) are important molecules that directly regulate gene expression. Transcription-related genes were obtained from the Cistrome Cancer database (http://cistrome.org),[12] a comprehensive resource for predicted TF targets in cancers. Next, differentially expressed transcription-related genes were intersected from DEGs. The criteria were set as log fold change greater than 1 and FDR value less than 0.05. Furthermore, correlation analysis between differentially expressed TFs and survival-associated IRGs was performed using the R psych package, and a correlation coefficient greater than 0.4 was considered significant. Finally, the regulatory network of identified IRGs and potential TFs was constructed using Cytoscape (version 3.7.1).

2.5. Construction of the immune-based risk signature

The risk score was calculated based on a linear combination of the Cox coefficient and gene expression. Patients were divided into high- and low-risk groups based on the median risk score, and survival curves were obtained using R survival and survminer packages. To validate the prognostic capability of the immune-related risk model, we analyzed the area under the curve (AUC) with the R software survivalROC package to evaluate survival differences between high- and low-risk groups. Univariate and multivariate Cox analyses were performed to assess the independent prognostic ability of the immune-related risk model.

2.6. Clinical utility of immune-based risk signature

Differences between the risk score and clinicopathological features, including age, sex, pathologic stage, and TNM stages, were performed. Tumor-infiltrating immune cells were downloaded from the TIMER database.[13] The relationship between tumor-infiltrating immune cells and risk score was assessed in tumor samples.

2.7. Construction and validation of the nomogram

A nomogram was constructed using the "rms," "Hmisc," "lattice," "Formula," and "foreign" R packages, and the

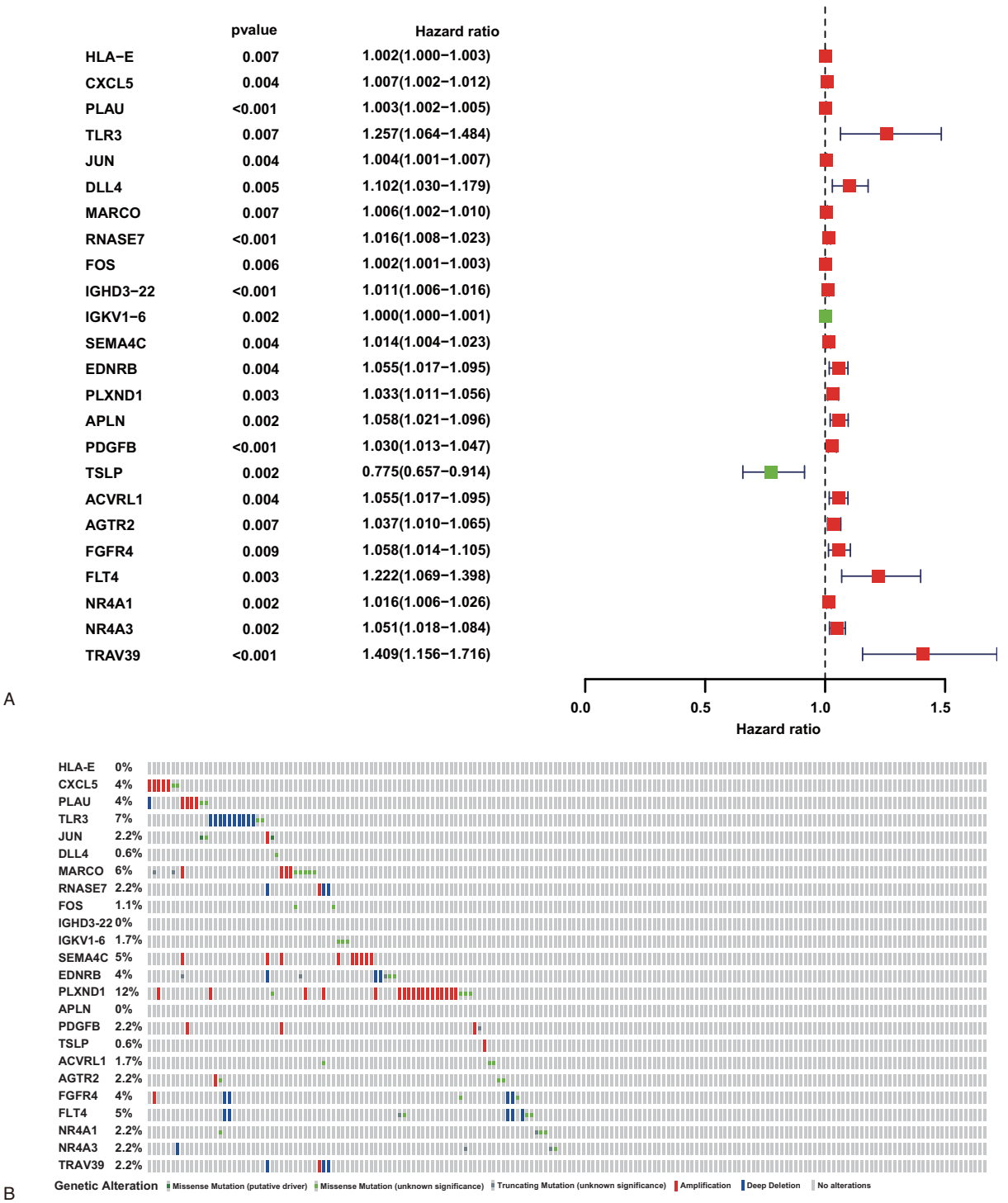

Figure 3. Characteristics of differentially expressed IRGs. (A) Forest plot of hazard ratios showing the survival-related IRGs. (B) Genetic alterations of survival-related IRGs. IRGs = immune-related genes.

corresponding calibration map was built to evaluate the prognostic performance of the nomogram. To validate the constructed novel nomogram, we performed decision curve analysis (DCA) to quantify its clinical applicability by analyzing the clinical outcomes of nomogram-based decisions.

2.8. Statistical analysis

Student *t* test was used to perform a statistical comparison. DEGs were visualized as a heatmap and volcano plot using the R heatmap and ggplot2 packages. Statistical significance was defined as an FDR < 0.05.

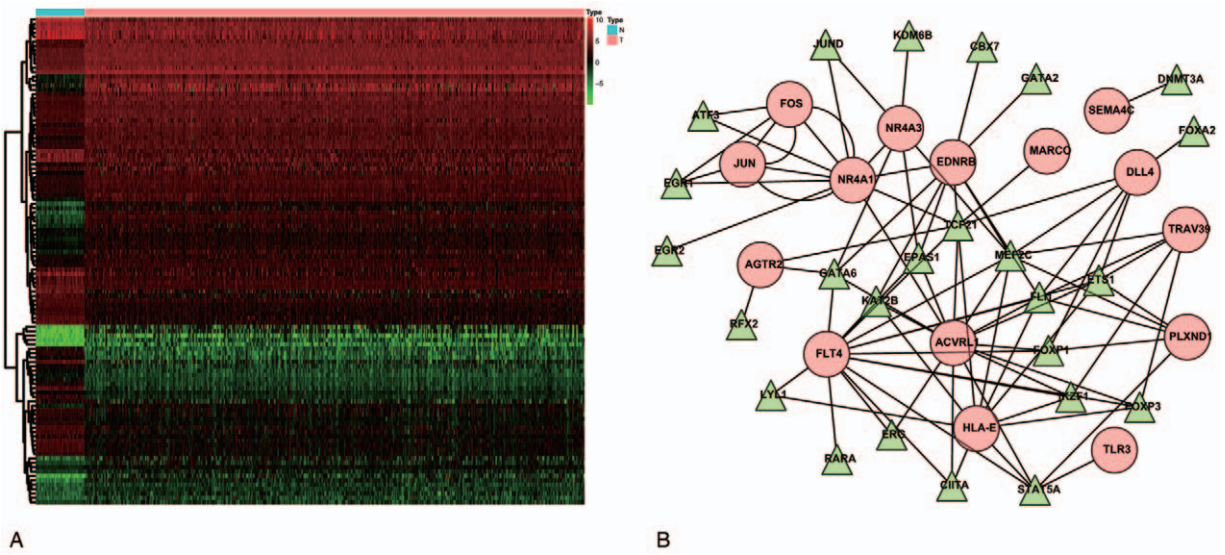

Figure 4. Construction of regulatory network. (A) Heatmap of differentially expressed TFs in lung squamous carcinoma. (B) Regulatory network constructed based on potentially relevant TFs and IRGs. IRGs = immune-related genes, TFs = transcriptional factors.

3. Results

3.1. Identification of differentially expressed IRGs

We identified 8468 DEGs, including 5993 upregulated and 2575 downregulated genes (Fig. 1A and C). From the DEG set, 593 differentially expressed IRGs, including 307 upregulated and 286 downregulated genes, were screened (Fig. 1B and D). Functional enrichment analysis revealed that the identified IRGs were mostly enriched in immune response, plasma membrane, growth factor activity, and cytokine-cytokine receptor interaction in terms of gene ontology (GO) and Kyoto Encyclopedia of Genes and Genomes (KEGG) pathways (Fig. 2).

3.2. Identification of survival-associated IRGs

To establish prognostic biomarkers at the molecular level, we investigated IRGs associated with survival in LUSC samples. A forest plot showed that 24 IRGs significantly correlated with OS, and most of these genes were risk factors with a hazard ratio greater than 1.0 (Fig. 3A). In addition, the percentages of genetic alterations in LUSC ranged from 0% to 12%, mostly including amplification and deep deletion (Fig. 3B).

3.3. Construction of the regulatory network

To explore the regulatory mechanisms of identified survival-associated IRGs at the transcriptional level, we collected 111 differentially expressed transcription-related genes between LUSC and control samples from the Cistrome database (Fig. 4A). Among these genes, 25 TFs positively regulated the 15 survival-associated IRGs in patients with LUSC and were visualized as regulatory networks (Fig. 4B).

3.4. Development of the immune-based risk signature

To determine the prognostic risk in patients with LUSC, we constructed an immune-based risk signature based on multivariate Cox regression results (Fig. 5). The risk score was calculated as follows: [(CXCL5) × 0.0065] + [(PLAU) × 0.0031] + [(RNASE7) × 0.0118] + [(IGHD3–22) × 0.0091] + [(IGKV1-6) × 0.0004] + [(SEMA4C) × 0.0146] +[(APLN) × 0.0523] + [(TSLP) × (− -0.2033)]+ [(FGFR4) × 0.0456] + [(TRAV39) × 0.3100]. The general characteristics of the IRGs in the risk signature are presented in Table 1. This immune-based prognostic signature could be a predictive tool for patients with LUSC based on clinical parameters (Fig. 6A). For the receiver operating characteristic (ROC) curve, the AUC was 0.661, suggesting a moderate capability of this signature for LUSC-specific survival (Fig. 6B). Univariate and multivariate Cox analyses revealed that the immune-based risk signature could serve as an independent predictor after adjusting for other clinicopathological features (Fig. 6C and D). In addition, the clinical significance of these identified genes was evaluated, and the differential expression of *APLN*, *FGFR4*, *PLAU*, *RNASE7*, and *SEMA4C* was observed in patients with various clinical features (Fig. 7).

3.5. Clinical significance of immune-based risk signature

To validate the clinical significance of the immune-based risk signature, we assessed the association between the risk score and clinicopathological features. The results showed that the high-risk score positively correlated only with elderly patients (Fig. 8). To explore the TIME, correlations between risk score and immune cell infiltration were analyzed. The results indicated that the risk score positively correlated with the infiltration of $CD8^+$ T cells, macrophages, neutrophils, and dendritic cells (Fig. 9).

3.6. Construction of a nomogram

As this novel IRG signature showed good predictive value for the LUSC prognosis, a more convenient and sensitive nomogram model, which included the IRG signature and pathological stage, age, and sex, was developed (Fig. 10A). The AUC values for the 1-, 3-, and 5-year OS predictions using the nomogram were 0.776,

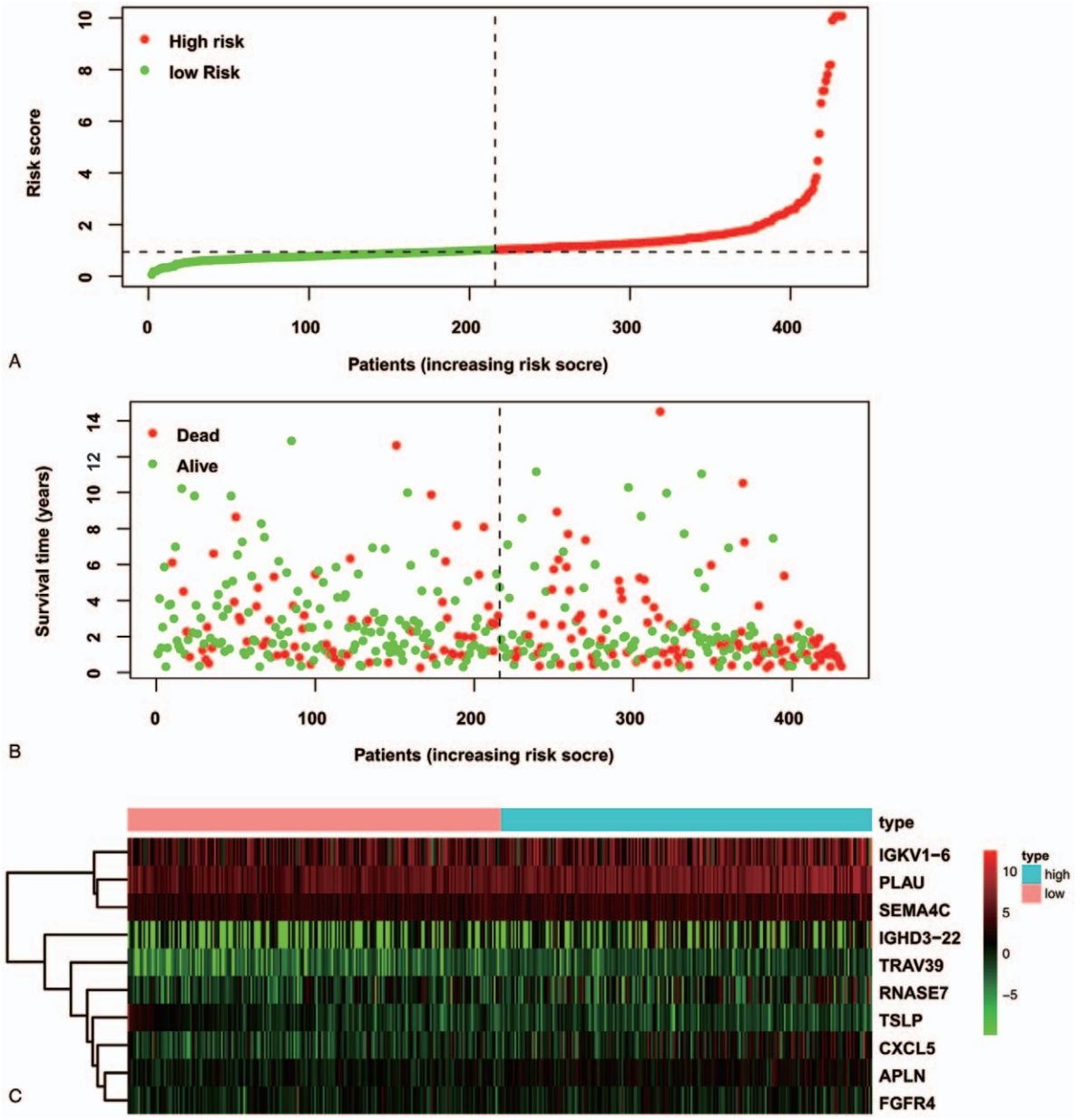

Figure 5. Development of the immune-based prognostic risk signature. (A) Rank of risk signature and distribution of groups. (B) Survival status of patients in low- and high-risk groups. (C) Heatmap of the expression profiles of the included genes.

Table 1

General characteristics of the IRGs in the risk signature.

	Differentially express			Multivariate analysis		
Gene symbol	LogFC	*P*	FDR	Coefficient	HR	*P*
CXCL5	−1.8119	3.29E-18	1.26E-17	0.0065	1.0065	.0217
PLAU	2.8381	7.23E-24	5.23E-23	0.0031	1.0031	.0003
RNASE7	5.6196	4.28E-18	1.63E-17	0.0118	1.0119	.0132
IGHD3-22	1.0962	.0258	0.0300	0.0091	1.0091	.0008
IGKV1-6	1.9339	.0007	0.0009	0.0004	1.0004	.0014
SEMA4C	1.0434	4.03E-15	1.19E-14	0.0146	1.0148	.0015
APLN	−2.963	1.03E-19	4.53E-19	0.0523	1.0537	.0038
TSLP	1.3356	.0004	0.0005	−0.2033	0.8160	.0164
FGFR4	−2.9544	1.33E-29	4.96E-28	0.0456	1.0467	.0229
TRAV39	−1.0823	2.42E-09	4.75E-09	0.3100	1.3635	.0056

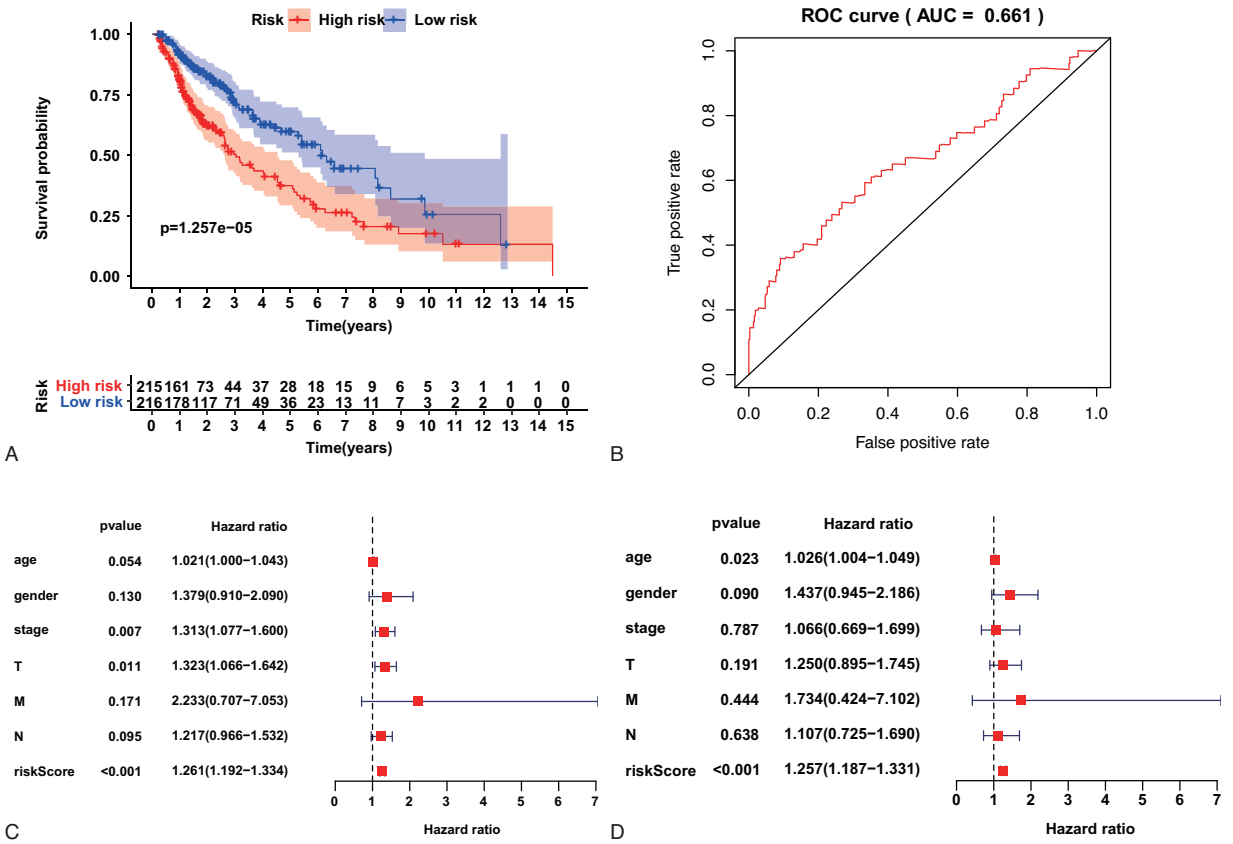

Figure 6. The prognostic value of risk signature and Cox regression analysis of lung squamous carcinoma. (A) Patients in the high-risk group demonstrate shorter overall survival. (B) Receiver operating characteristic (ROC) curve showing the prognostic value of the risk signature. (C) Univariate Cox regression analysis of discrete clinical factors. (D) Multivariate Cox regression analysis of discrete clinical factors.

0.787, and 0.762, respectively (Fig. 10B). Calibration plots based on the training set revealed that the nomogram could accurately predict 1-, 3-, and 5-year OS (Fig. 10C). In addition, DCA was performed for the nomogram and TNM stage, indicating the marked clinical usefulness of this model (Fig. 10D).

4. Discussion

LUSC is a heterogeneous disease with no effective treatments owing to its complex genomic pattern. More recently, a key role has been credited to the tumor immune response in the pathogenesis and progression of LUSC.[14,15] From this perspective, some researchers have reported that a risk signature based on immunogenomic or immune infiltrating cells could be an independent prognostic factor for NSCLC, especially adenocarcinomas.[16–18] In the present study, we aimed to develop an immunogenomic prognostic signature in LUSC and provide evidence regarding the role of the immunogenomic signature to predict clinical outcomes in this disease.

Ten IRGs (*IGKV1-6, PLAU, SEMA4C, IGHD3-22, TRAV39, RNASE7, TSLP, CXCL5, APLN,* and *FGFR4*) were selected from 24 survival-related IRGs to construct the risk signature. As expected, this signature can distinguish high-risk patients with LUSC and predict OS. Furthermore, this risk signature may act as a reliable and independent prognostic factor. To investigate the clinical utility of the risk signature based on IRGs, we analyzed the differential expression of these 10 IRGs in patients with various clinical features.

Apelin (APLN), a ligand of the APJ receptor that belongs to the G protein coupled receptor family, is considered an angiogenic factor and has a potential role in tumor angiogenesis.[19] Accumulated evidence has demonstrated that APLN overexpression significantly correlates with worse OS in patients with NSCLC.[20,21] Fibroblast growth factor receptor 4 (FGFR4) plays an essential role in the tumor microenvironment and is linked to oncogenesis, which is associated with prognosis in LUSC.[22–24] Semaphorin 4C (SEMA4C) reportedly regulates immune cell interactions, angiogenesis, and tumor growth.[25] A previous study has shown that SEMA4C knockdown inhibits NSCLC cell proliferation and reverses epithelial-mesenchymal transition.[26] In the present study, APLN expression was significantly elevated in LUSC patients aged > 65 years, and the levels of FGFR4 and SEMA4C were increased in male LUSC patients without metastasis. Combined with previous studies, these 3 genes may act as risk factors for LUSC. The levels of unexplored genes (PLAU and RNASE7) significantly correlated with age, tumor stage, and TNM status. In addition, the expression of these genes can be regulated by transcription factors, such as Foxp3, which plays a crucial role in the maintenance of cancer immune homeostasis.[27] These results suggest that identified IRGs or TFs could be novel biomarkers or therapeutic targets for LUSC. The risk signature was significantly

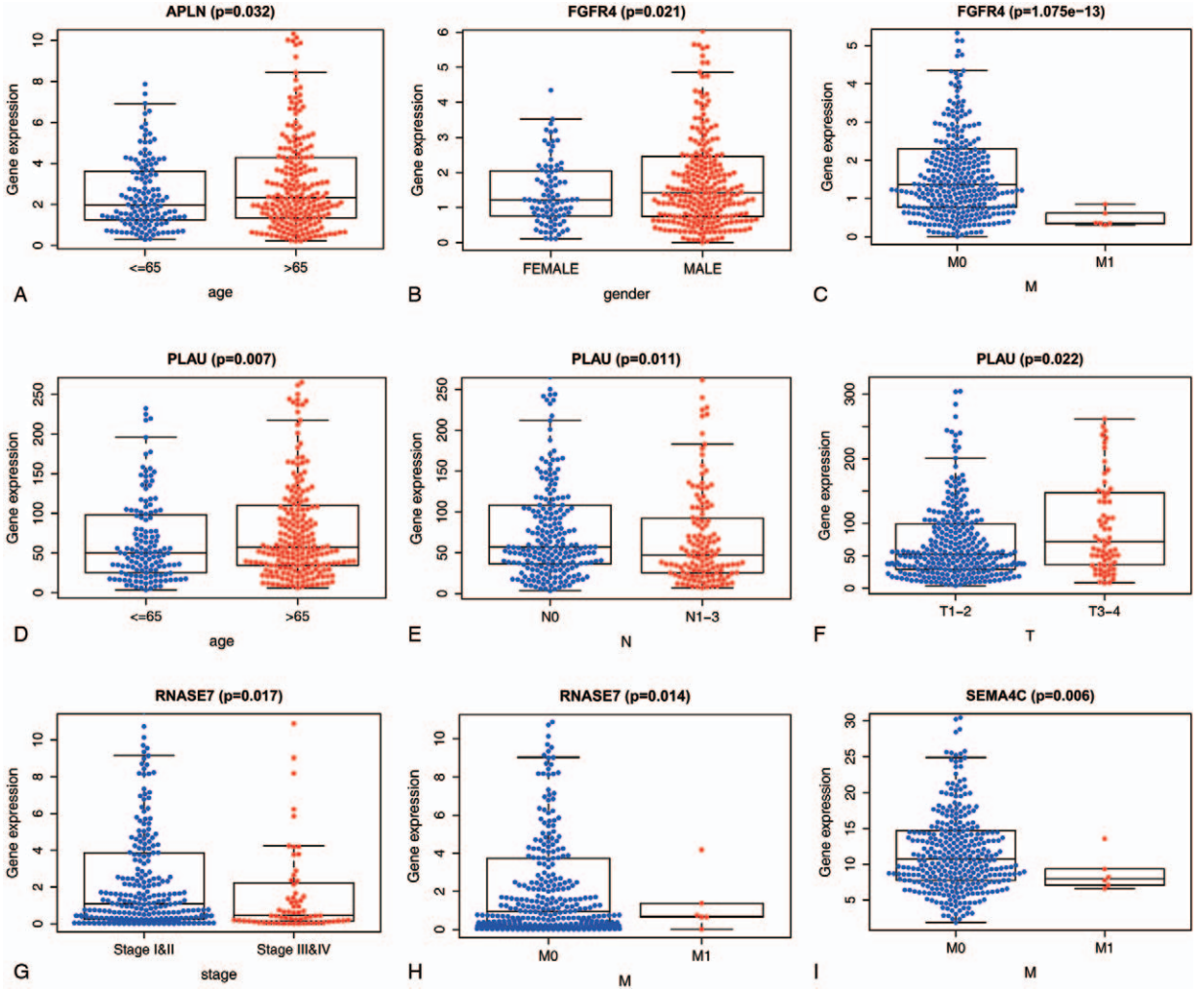

Figure 7. The differential expression of immune-based IRGs in patients with varied clinical features such as age, gender, tumor stage, and TNM status. IRGs = immune-related genes.

associated with age, suggesting a robust prognostic tool for elderly patients.

To explore the underlying molecular mechanisms of IRGs, functional enrichment analysis revealed that IRGs were mainly enriched in the immune response, inflammatory response, and cytokine-cytokine receptor interaction. Growing evidence has demonstrated that coordinating adaptive or innate immune responses is a promising therapy against various tumors, and benefits from immunotherapy have been achieved in patients with cancer.[28,29] It is well-established that inflammatory cytokines are actively involved in the tumorigenesis, aggression, and metastasis of LUSC, suggesting that these cytokines could act as clinical biomarkers for monitoring disease or therapeutic targets.[30,31] Furthermore, the majority of IRGs present genetic alterations, including amplification and deep deletion, and these genomic discoveries were found to be associated with clinical outcomes.[32]

Emerging evidence has revealed that cancer immune infiltrating cells are closely correlated with clinical outcomes.[33,34] In this study, we investigated the correlation between risk signature and immune infiltrating cells. Notably, the risk score positively correlated with the infiltration of $CD8^+$ T cells, macrophages, neutrophils, and dendritic cells, indicating that the levels of these four immune cells might be elevated in high-risk patients and that the signature could be a predictor for immune cell infiltration. Previously, a study has reported that early proliferative $CD8\ T^+$ cell responses are associated with favorable prognosis in NSCLC patients with PD-1 targeted therapy.[35] Tumor-immune infiltrating cells are mostly composed of macrophages, which demonstrate distinct effects on oncogenesis depending on their polarization within the TIME.[36] Studies have consistently reported that macrophage density and phenotype are closely associated with survival in patients with LUSC.[37,38]

Nonetheless, there are some limitations to the present study. The risk signature was constructed based on retrospective data and was not validated using another independent cohort. Thus, clinical validation using prospective samples is needed to test the potential of this signature. Moreover, the molecular functions of the included IRGs require further biological experiments.

Collectively, this novel signature could be used as a prognostic tool for LUSC and a potential predictor of the immune status in patients with LUSC. Large-scale, well-controlled translational studies are needed to evaluate the therapeutic implications of immunogenomics.

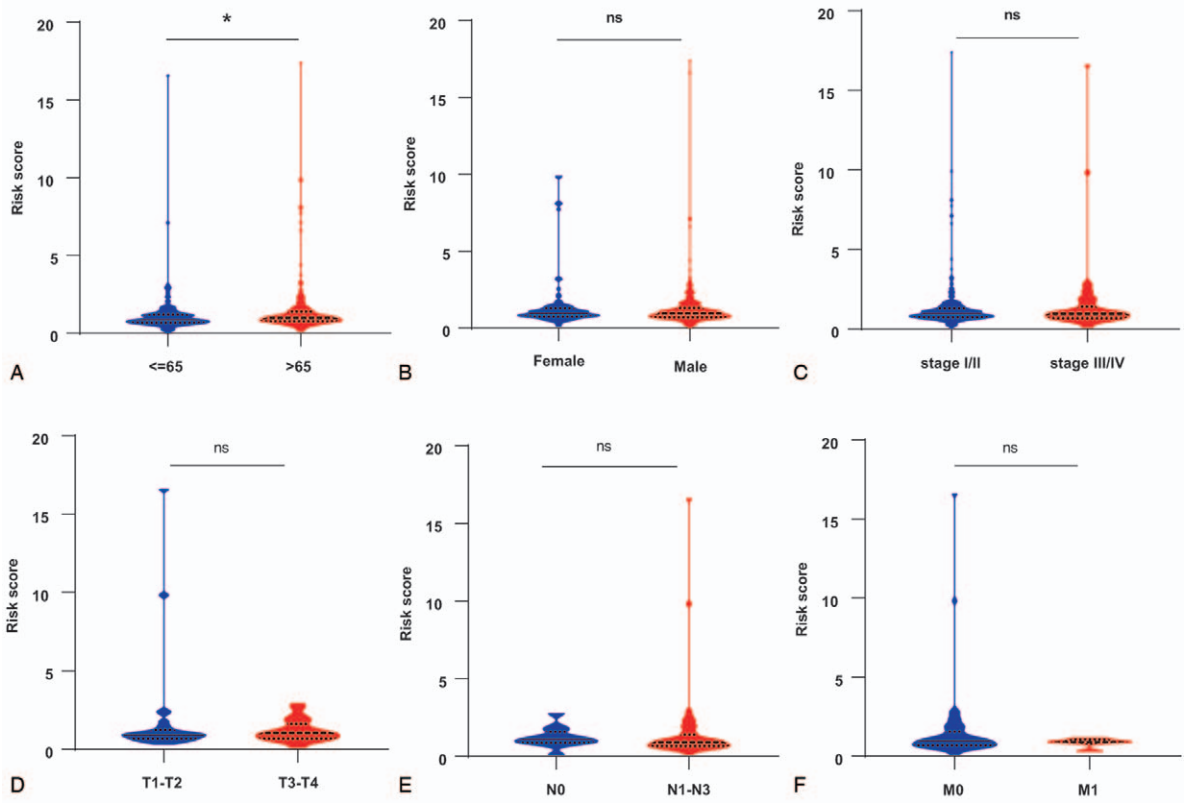

Figure 8. The relationships between the immune-based risk signature and (A) age; (B) gender; (C) tumor stage; (D) TNM stage; (E) lymph node metastasis; and (F) distant metastasis. ns, no statistical significance; $^{*}P < .05$.

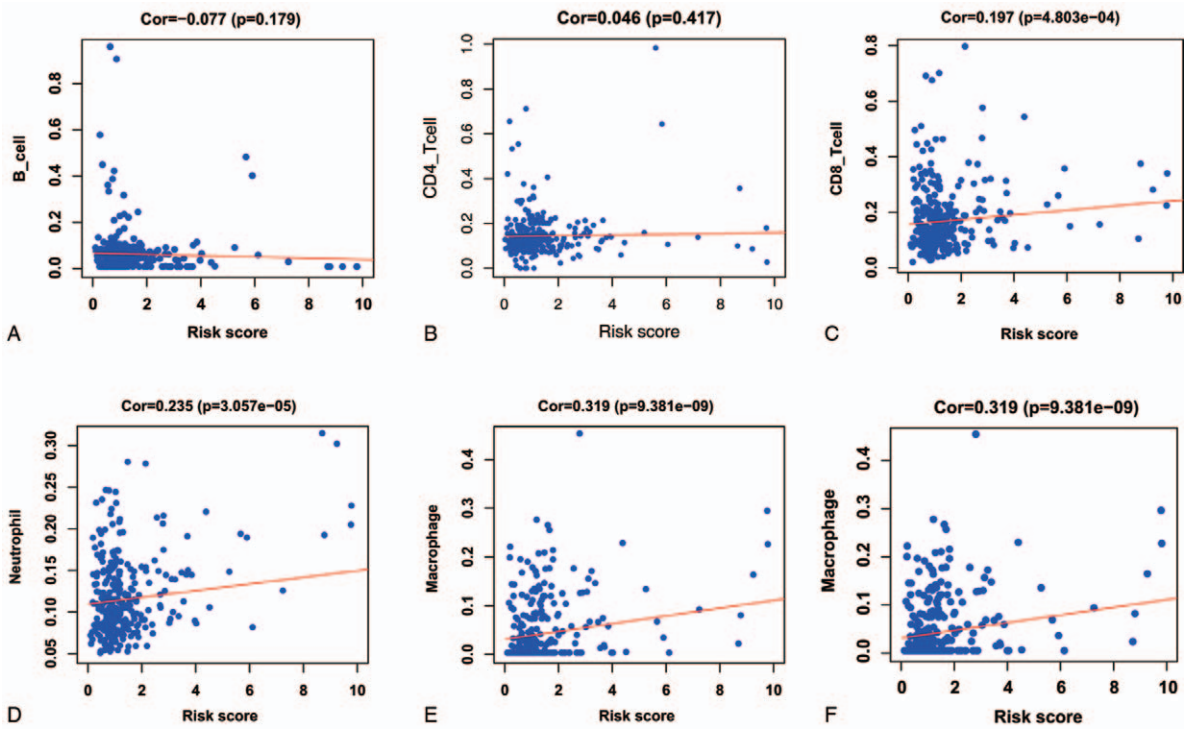

Figure 9. The correlation between the immune-based risk signature and immune infiltrating cells, including B cells, $CD4^{+}$ T cells, $CD8^{+}$ T cells, macrophages, neutrophils, and dendritic cells.

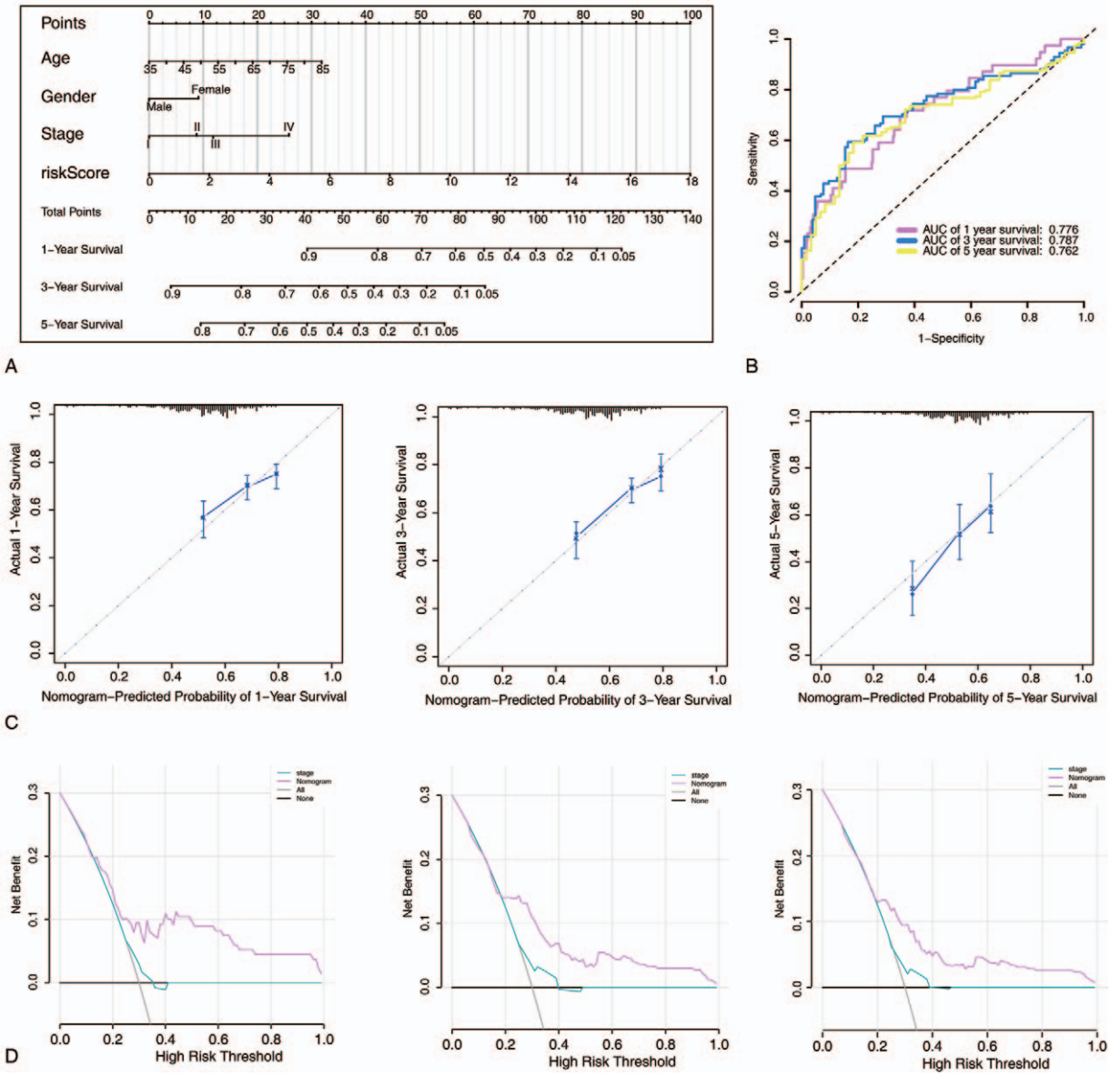

Figure 10. Construction of a nomogram based on the IRG signature. (A) Nomogram based on the IRG signature and clinical information of patients with LUSC. (B) ROC curves of the nomogram for predicting OS. (C) Calibration plot of the nomogram for predicting OS. (D) DCA of the nomogram for predicting OS. DCA = decision curve analysis, IRG = immune-related genes, LUSC = lung squamous carcinoma, OS = overall survival, ROC = receiver operating characteristic.

Author contributions

Data curation: Jili Hou, Qiuying Zhong.
Formal analysis: Qiuying Zhong.
Methodology: Jili Hou, Qiuying Zhong.
Supervision: Jili Hou, Qiuying Zhong.
Writing – original draft: Jili Hou.
Writing – review & editing: Qiuying Zhong.

References

[1] Bray F, Ferlay J, Soerjomataram I, et al. Global cancer statistics 2018: GLOBOCAN estimates of incidence and mortality worldwide for 36 cancers in 185 countries. CA Cancer J Clin 2018;68:394–424.
[2] van Meerbeeck JP, Fennell DA, De Ruysscher DKM. Small-cell lung cancer. Lancet (London, England) 2011;378:1741–55.
[3] Wu YL, Planchard D, Lu S, et al. Pan-Asian adapted Clinical Practice Guidelines for the management of patients with metastatic non-small-cell lung cancer: a CSCO-ESMO initiative endorsed by JSMO, KSMO, MOS, SSO and TOS. Ann Oncol 2019;30:171–210.
[4] Okamoto T, Takada K, Sato S, et al. Clinical and genetic implications of mutation burden in squamous cell carcinoma of the lung. Ann Surg Oncol 2018;25:1564–71.
[5] Xu X, Huang Z, Zheng L, et al. The efficacy and safety of anti-PD-1/PD-L1 antibodies combined with chemotherapy or CTLA4 antibody as a first-line treatment for advanced lung cancer. Int J Cancer 2018;142:2344–54.
[6] Hellmann MD, Rizvi NA, Goldman JW, et al. Nivolumab plus ipilimumab as first-line treatment for advanced non-small-cell lung cancer (CheckMate 012): results of an open-label, phase 1, multicohort study. Lancet Oncol 2017;18:31–41.
[7] Öjlert ÅK, Halvorsen AR, Nebdal D, et al. The immune microenvironment in non-small cell lung cancer is predictive of prognosis after surgery. Mol Oncol 2019;13:1166–79.

[8] Meng X, Gao Y, Yang L, et al. Immune microenvironment differences between squamous and non-squamous non-small-cell lung cancer and their influence on the prognosis. Clin Lung Cancer 2019;20:48–58.
[9] Mollaoglu G, Jones A, Wait SJ, et al. The lineage-defining transcription factors SOX2 and NKX2-1 determine lung cancer cell fate and shape the tumor immune microenvironment. Immunity 2018;49:764–79.e9.
[10] Bhattacharya S, Andorf S, Gomes L, et al. ImmPort: disseminating data to the public for the future of immunology. Immunol Res 2014;58:234–9.
[11] Cerami E, Gao J, Dogrusoz U, et al. The cBio cancer genomics portal: an open platform for exploring multidimensional cancer genomics data. Cancer Discov 2012;2:401–4.
[12] Mei S, Meyer CA, Zheng R, et al. Cistrome cancer: a web resource for integrative gene regulation modeling in cancer. Cancer Res 2017;77:e19–22.
[13] Li T, Fan J, Wang B, et al. TIMER: a web server for comprehensive analysis of tumor-infiltrating immune cells. Cancer Res 2017;77:e108–10.
[14] Faruki H, Mayhew GM, Serody JS, et al. Lung adenocarcinoma and squamous cell carcinoma gene expression subtypes demonstrate significant differences in tumor immune landscape. J Thorac Oncol 2017;12:943–53.
[15] Campbell JD, Alexandrov A, Kim J, et al. Distinct patterns of somatic genome alterations in lung adenocarcinomas and squamous cell carcinomas. Nat Genet 2016;48:607–16.
[16] Song Q, Shang J, Yang Z, et al. Identification of an immune signature predicting prognosis risk of patients in lung adenocarcinoma. J Transl Med 2019;17:70.
[17] Song P, Guo L, Li W, et al. Clinicopathologic correlation with expression of PD-L1 on both tumor cells and tumor-infiltrating immune cells in patients with non-small cell lung cancer. J Immunother 2019;42:23–8.
[18] Li B, Cui Y, Diehn M, et al. Development and validation of an individualized immune prognostic signature in early-stage nonsquamous non-small cell lung cancer. JAMA Oncol 2017;3:1529–37.
[19] Uribesalgo I, Hoffmann D, Zhang Y, et al. Apelin inhibition prevents resistance and metastasis associated with anti-angiogenic therapy. EMBO Mol Med 2019;11:e9266.
[20] Zhou Y, Zhao M, Du Y, et al. MicroRNA-195 suppresses the progression of lung adenocarcinoma by directly targeting apelin. Thorac Cancer 2019;10:1419–30.
[21] Berta J, Kenessey I, Dobos J, et al. Apelin expression in human non-small cell lung cancer: role in angiogenesis and prognosis. J Thorac Oncol 2010;5:1120–9.
[22] Quintanal-Villalonga A, Molina-Pinelo S, Yagüe P, et al. FGFR4 increases EGFR oncogenic signaling in lung adenocarcinoma, and their combined inhibition is highly effective. Lung Cancer 2019;131:112–21.
[23] Quintanal-Villalonga Á, Carranza-Carranza A, Meléndez R, et al. Prognostic role of the FGFR4-388Arg variant in lung squamous-cell carcinoma patients with lymph node involvement. Clin Lung Cancer 2017;18:667–74.e1.
[24] Hibi M, Kaneda H, Tanizaki J, et al. FGFR gene alterations in lung squamous cell carcinoma are potential targets for the multikinase inhibitor nintedanib. Cancer Sci 2016;107:1667–76.
[25] Zeng R, Han M, Luo Y, et al. Role of Sema4C in TGF-(1-induced mitogen-activated protein kinase activation and epithelial-mesenchymal transition in renal tubular epithelial cells. Nephrol Dial Transplant 2011;26:1149–56.
[26] Li J, Wang Q, Wen R, et al. MiR-138 inhibits cell proliferation and reverses epithelial-mesenchymal transition in non-small cell lung cancer cells by targeting GIT1 and SEMA4C. J Cell Mol Med 2015;19:2793–805.
[27] Wing JB, Tanaka A, Sakaguchi S. Human FOXP3 regulatory T cell heterogeneity and function in autoimmunity and cancer. Immunity 2019;50:302–16.
[28] Schmidt L, Eskiocak B, Kohn R, et al. Enhanced adaptive immune responses in lung adenocarcinoma through natural killer cell stimulation. Proc Natl Acad Sci U S A 2019;116:17460–9.
[29] Benci JL, Johnson LR, Choa R, et al. Opposing functions of interferon coordinate adaptive and innate immune responses to cancer immune checkpoint blockade. Cell 2019;178:933–84.e14.
[30] Barrera L, Montes-Servín E, Barrera A, et al. Cytokine profile determined by data-mining analysis set into clusters of non-small-cell lung cancer patients according to prognosis. Ann Oncol 2015;26:428–35.
[31] Shiels MS, Pfeiffer RM, Hildesheim A, et al. Circulating inflammation markers and prospective risk for lung cancer. J Natl Cancer Inst 2013;105:1871–80.
[32] Presley CJ, Tang D, Soulos PR, et al. Association of broad-based genomic sequencing with survival among patients with advanced non-small cell lung cancer in the community oncology setting. JAMA 2018;320:469–77.
[33] Sun R, Limkin EJ, Vakalopoulou M, et al. A radiomics approach to assess tumour-infiltrating CD8 cells and response to anti-PD-1 or anti-PD-L1 immunotherapy: an imaging biomarker, retrospective multi-cohort study. Lancet Oncol 2018;19:1180–91.
[34] Gentles AJ, Newman AM, Liu CL, et al. The prognostic landscape of genes and infiltrating immune cells across human cancers. Nat Med 2015;21:938–45.
[35] Kamphorst AO, Pillai RN, Yang S, et al. Proliferation of PD-1+ CD8 T cells in peripheral blood after PD-1-targeted therapy in lung cancer patients. Proc Natl Acad Sci U S A 2017;114:4993–8.
[36] Conway EM, Pikor LA, Kung SHY, et al. Macrophages, inflammation, and lung cancer. Am J Respir Crit Care Med 2016;193:116–30.
[37] Tseng Y-H, Ho H-L, Lai C-R, et al. PD-L1 expression of tumor cells, macrophages, and immune cells in non-small cell lung cancer patients with malignant pleural effusion. J Thorac Oncol 2018;13:447–53.
[38] Dai F, Liu L, Che G, et al. The number and microlocalization of tumor-associated immune cells are associated with patient's survival time in non-small cell lung cancer. BMC Cancer 2010;10:220.